Theor Chem Acc (2011) 128:457–464
DOI 10.1007/s00214-010-0801-z

REGULAR ARTICLE

Assisted intramolecular proton transfer in $(uracil)_2Ca^{2+}$ complexes

Ane Eizaguirre · Al Mokhtar Lamsabhi · Otilia Mó · Manuel Yáñez

Received: 2 June 2010 / Accepted: 18 August 2010 / Published online: 9 September 2010

Abstract The structure and relative stability of the complexes between uracil dimers and Ca^{2+}, as well as the proton transfer (PT) processes within these dimers, have been investigated by the density functional theory methods. Although in uracil dimers PT occurs as an almost synchronous double PT processes that connect the diketo dimer with a keto-enol dimer, the process within the most stable $(uracil)_2Ca^{2+}$ complexes is much more complicated, and the product of the reaction looks like the result of an intramolecular PT from one of the NH groups of one monomer to one of the carbonyl groups of the same monomer. An analysis of the force profile along the reaction coordinate shows that the intimate mechanism implies three elementary steps, two intermolecular PTs, and an in-plane displacement of one monomer with respect to the other. The result of this so-called assisted intramolecular proton transfer is the formation of a dimer in which only one monomer is a keto-enol derivative, the other monomer being apparently unchanged, although it suffers significant structural rearrangements along the reaction coordinate. Quite importantly, this dimer is significantly stabilized upon Ca^{2+} association; therefore, while the most stable uracil dimers correspond systematically to associations involving only the diketo forms, in $(uracil)_2Ca^{2+}$ complexes the most stable structures correspond to those in which one of the monomers is a keto-enol uracil isomer.

Keywords Uracil dimers · Proton transfer · Ca^{2+} complexes · DFT calculations · Reaction force analysis

1 Introduction

Watson–Crick base pairs [1, 2] have received a great deal of attention along many decades because they are the building blocks of DNA and RNA [3, 4]. These pairs are held together by a network of intermolecular hydrogen bonds which are crucial in the transmission of the genetic information [5]. It is believed that some of these mutagenic and mispairing processes may have their origin in proton transfer (PT) mechanisms [6] taking place from one monomer of the base pair to the other, which produce new tautomeric forms and therefore permanent alterations of the base pair and an incorrect transmission of the genetic information. Therefore, these PT processes have been the subject of both experimental and theoretical analysis [7–22].

Among the aforementioned bases, uracil and its thio and seleno derivatives have received particular attention because they exhibit a large number of keto-enol tautomeric forms, [23–33] and because they are involved in many biochemical process playing an important role in the t-RNA helices stability. The tautomeric forms of uracil could be generated through intramolecular PT within the molecule, but these processes require very large activation barriers are not likely to occur. On the other hand, it is well established that the most stable conformation of uracil corresponds to its diketo form. Much more favorable processes leading from the diketo form of uracil to some keto-enol tautomer are intermolecular PTs within the dimer,

Published as part of the special issue celebrating theoretical and computational chemistry in Spain.

Electronic supplementary material The online version of this article (doi:10.1007/s00214-010-0801-z) contains supplementary material, which is available to authorized users.

A. Eizaguirre · A. M. Lamsabhi · O. Mó (✉) · M. Yáñez
Departamento de Química, Módulo 13, Universidad Autónoma de Madrid, Cantoblanco, Campus de Excelencia UAM-CSIC, 28049 Madrid, Spain
e-mail: otilia.mo@uam.es

which required much lower barriers than the intramolecular PTs within the monomers, because the mechanisms actually involves a double PT from one monomer to the other [34]. It has also been shown that for the particular case of uracil these double PT are practically synchronous processes, whereas for the thiouracil derivatives they exhibit some degree of asynchronicity [34]. The question we want to analyze in this paper is, "are there any possible effects that the interaction of the base pair with metal ions may have in these double PT processes?" For this purpose, we have chosen Ca^{2+} because (1) the perturbation of the base will be more significant when interacting with a doubly charged species than with singly charged cations (2) Ca^{2+} is ubiquitous in physiological media, and (3) differently to other doubly charged metal ions, such as Cu^{2+} [35] or Pb^{2+} [36], Ca^{2+} [37] does not lead to a spontaneous deprotonation of the base.

Several studies on the interaction of base pairs with doubly charged metal ions and in particular with alkaline-earth cations have been reported in the literature, [21, 38–40] but much less attention was paid to the effects of this association on the tautomerization processes which may take place within the base pair [21, 32, 36].

2 Computational details

The geometries of the different uracil dimers and their complexes with Ca^{2+} were optimized by using the hybrid B3LYP functional. This approach, which combines the nonlocal correlation function of Lee et al. [41] with the Becke's three-parameter nonlocal hybrid exchange functional [42], has been shown to provide very reliable geometries and harmonic vibrational frequencies for a great variety of systems. Furthermore, in previous theoretical assessments, it has been shown to be a very good compromise between accuracy and computational effort when dealing with Ca^{2+} interactions [43]. This approach, when used with flexible enough basis sets, also performs quite well in describing both inter- and intramolecular hydrogen bonds, which in our case are important actors in the mechanisms to be investigated. It must be mentioned, however, that in a recent assessment using adenine-thymine and guanine-cytosine base pairs as model system it was found that B3LYP method slightly overestimated hydrogen bond distances when compared with MP2 ones [44]. Geometry optimizations and harmonic vibrational frequencies were evaluated using a DZ-polarized 6-31 + G(d,p) basis set expansion, which includes diffuse functions on the heavy atoms, required to an appropriate description of hydrogen bonding and the polarization effects induced by the doubly charged metal ion on the base. The harmonic vibrational frequencies so obtained were used to evaluate the vibrational thermal corrections and classify the stationary points located on the potential energy surface as local minima or transition states. To have reliable final energies, these were obtained in single-point calculations using a much larger 6-311 + G(3df,2p) basis set expansion.

The reaction force analysis [45–47] has been shown to offer interesting insights into the double PT mechanisms within uracil dimers and therefore we have decided to apply the same approach for the analysis of similar processes within $(uracil)_2Ca^{2+}$ complexes.

The lowest energy path connecting reactants and products in an elementary reaction when projected into the intrinsic reaction coordinate typically presents a maximum corresponding to the transition state (TS) relying reactants and products. The differentiation of this energy curve leads to the reaction force,

$$F(\xi) = -\frac{\mathrm{d}E(\xi)}{\mathrm{d}\xi} \tag{1}$$

which presents two extrema, ξ_1 (minimum) and ξ_2 (maximum) (See Fig. 1), which in turn permit the identification of different regions with a well-defined chemical meaning [48, 49], namely (1) the reactant region ($\xi_R \leq \xi \leq \xi_1$) where the reactants begin to start activated by a negative retarding force, (2) the transition state region ($\xi_1 \leq \xi \leq \xi_2$) where a driving force increasingly balances the aforementioned retarding one, and (3) the products region ($\xi_2 \leq \xi \leq \xi_P$) where the system relaxes and the driving force tends to zero when approaching ξ_P. This partitioning of the reaction coordinate in different reaction regions allows dividing the activation energy into two main contributions, [49, 50]

$$\Delta E^{\#} = W_1 + W_2 \tag{2}$$

where,

$$W_1 = -\int_{\xi_R}^{\xi_1} F(\xi)\mathrm{d}\xi \quad \text{and} \quad W_2 = -\int_{\xi_1}^{\xi_0} F(\xi)\mathrm{d}\xi \tag{3}$$

In our particular case, the first term of Eq. 2 represents the work to be done to bring the HB donor and the HB acceptor close enough as to propitiate the PT process, whereas the second term corresponds to the energy required to reach the TS, in order to begin the evolution toward the products. Analogously, the second part of the reaction coordinate can be split into two components, W_3 and W_4, so that the reaction energy can be written as

$$\Delta E^0 = W_1 + W_2 + W_3 + W_4 \tag{4}$$

where W_3 represents the energy gaining on the relaxation of the system from the TS to ξ_2 and W_4 the energy to finally reach the products, and are given by

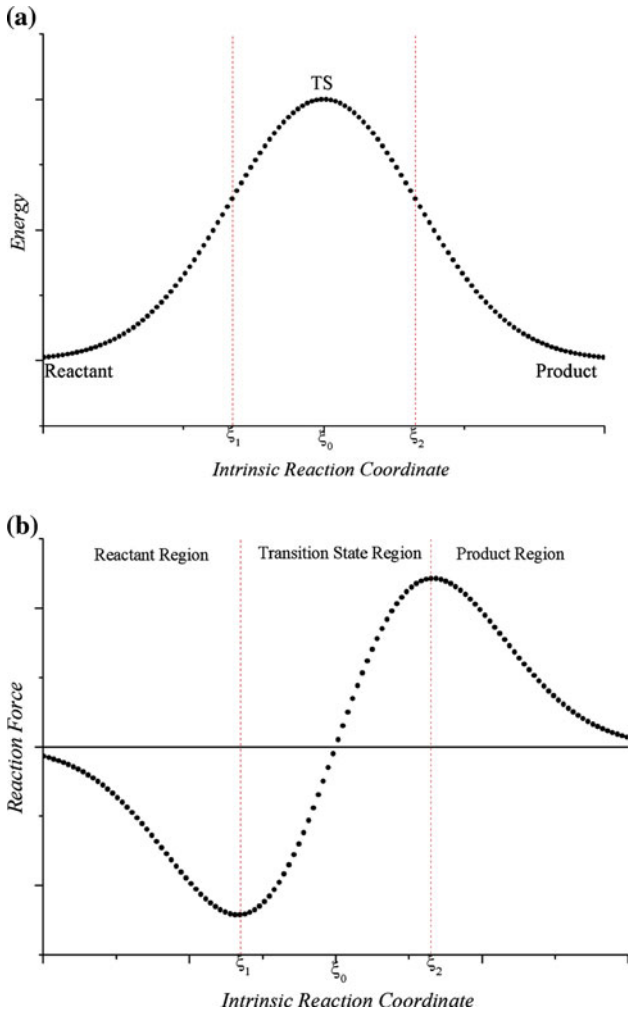

Fig. 1 Energy (**a**) and force (**b**) profiles for an elementary reaction connecting reactants (**R**) and products (**P**)

$$W_3 = -\int_{\xi_0}^{\xi_2} F(\xi)\mathrm{d}\xi \quad \text{and} \quad W_4 = -\int_{\xi_2}^{\xi_P} F(\xi)\mathrm{d}\xi \tag{5}$$

To carry out this analysis, the necessary calculations along the intrinsic reaction coordinate (IRC) expressed in mass-weighted cartesian coordinates, which involve a full geometry optimization at each step along ξ, were carried out as implemented in the Gaussian03 suite of programs.

The bonding perturbations triggered by the metal dication in the base pair were analyzed by means of the atoms in molecules (AIM) [51] and the electron localization function (ELF) [52, 53] theories. Within the framework of the former, we have evaluated the electron density at the different bond critical points (BCPs) and we have examined its evolution along the reaction coordinate by using the AIMALL series of programs [54]. The bonding changes in a system triggered by its interaction with a charged species can be also followed by analyzing the changes in the energy density

$$h(\vec{r}) = v(\vec{r}) + g(\vec{r}) \tag{6}$$

where $v(\vec{r})$ and $g(\vec{r})$ are the local densities of the kinetic energies, respectively. The regions in which this magnitude is negative or positive correspond to areas in which the electron density is built up or depleted, respectively, so that the former can be associated with covalent interactions, whereas the latter are typically associated with closed-shell interactions, as in ionic bonds or hydrogen bonds.

The ELF allows the partition of the molecular space into basins, [53, 55] usually disynaptic and monosynaptic, which correspond to regions of maximum probability of finding electron pairs. This description in terms of disynaptic basins, associated with bonding pairs, and monosynaptic basins, associated with lone-pairs or core-pair electrons, provides useful information about the nature of the bonding, even in challenge cases in which other approaches fail to give an unambiguous bonding picture [56]. The electron population within these basins can be obtained by integration of the electron density within the basins limits. ELF grids and basin integrations have been evaluated with the TopMod package [57]. For the three-dimensional plots, an ELF value of 0.8 has been used.

A complementary viewpoint some times crucial to understand the bonding can be obtained through the use of the NBO (Natural Bond Orbital) approach [58], which describes the bonding in terms of localized hybrids obtained as local block eigenvectors of the one particular density matrix. A second-order perturbation treatment permits also to quantify the interaction energies between occupied and virtual orbitals reflected in a charge transfer from the former to the latter. These kind of interactions are typically found in XH···Y hydrogen bonds, which are characterized by a charge transfer from the lone-pairs of the HB acceptor Y, to the antibonding σ_{XH}* orbital of the HB donor, XH [58].

3 Results and discussion

As it has been previously shown in the literature, uracil leads to six different dimers [59] (see Fig. 2), depending on the relative positions of the two monomers and the kind of hydrogen bonds connecting them. For instance, if we identify within the uracil molecule, a urea-like subunit (HN–CO–NH), and a formamide-like subunit (HN–CO–CH), it can be observed that for the global minimum, UU1, and the less stable dimers, UU3 and UU6, the HBs connecting both monomers, looking at the carbonyl groups which act as HB acceptors, correspond to a urea–urea interaction, the only difference between the three

complexes being the relative orientation of both monomers. UU2 and UU5 are connected through urea–formamide interactions and again only differ in the relative orientation of both monomers. Finally, UU4 dimer involves a formamide–formamide interaction.

The number of $(uracil)_2Ca^{2+}$ complexes is much larger since the metal dication can be attached to different basic sites of the dimer, but more importantly, the relative stability of the $(uracil)_2Ca^{2+}$ complexes does not reflect the relative stability of the uracil dimers. Actually, as shown in Fig. 2, the most stable $(uracil)_2Ca^{2+}$ complex, namely UU5-a, is formed by the association of Ca^{2+} to the one of the less stable uracil dimer (UU5). Conversely, the global minimum of the neutral dimers, UU1, leads upon Ca^{2+} association to one of the less stable $(uracil)_2Ca^{2+}$ complexes (UU1-a), 172 kJ mol^{-1} above UU5-a. It is also worth noting that in UU5-a, Ca^{2+} bridges between the two formamide-like carbonyl groups. Interestingly, when the metal dication interacts with the two urea-like carbonyl groups, the complex formed, UU5-b, is found to be 57 kJ mol^{-1} less stable. This can be easily explained if one takes into account that, as has been shown previously in the literature, the most basic site of the uracil molecule is the carbonyl group at position 4, so in complex UU5-a, Ca^{2+} interacts with the most basic site of both monomers, whereas in UU5-b complex it interacts with the least basic site centers. Although many other $(uracil)_2Ca^{2+}$ complexes have been calculated in our work, in Fig. 2 only the more stable ones are shown. Their total energies together with the zero point energy (ZPE) corrections are reported in Table S1 of the supporting information. The next important question to be addressed in this study, once we have located the global minimum of the $(uracil)_2Ca^{2+}$ PES, is the mechanism of the PT process in this complex, UU5-a.

4 Proton transfer processes

As mentioned in the introduction, in uracil dimers, the most favorable PT process corresponds to a practically synchronous double PT mechanism, [34] so that the product is a dimer in which both interacting monomers are enolic forms of uracil. As illustrated in Fig. 3, the situation seems to be significantly different upon the interaction with Ca^{2+}, where the product arises formally from an intramolecular PT process in which the proton is transferred from a NH group of one monomer toward the carbonyl group of the same monomer. The result is that, after the PT, the

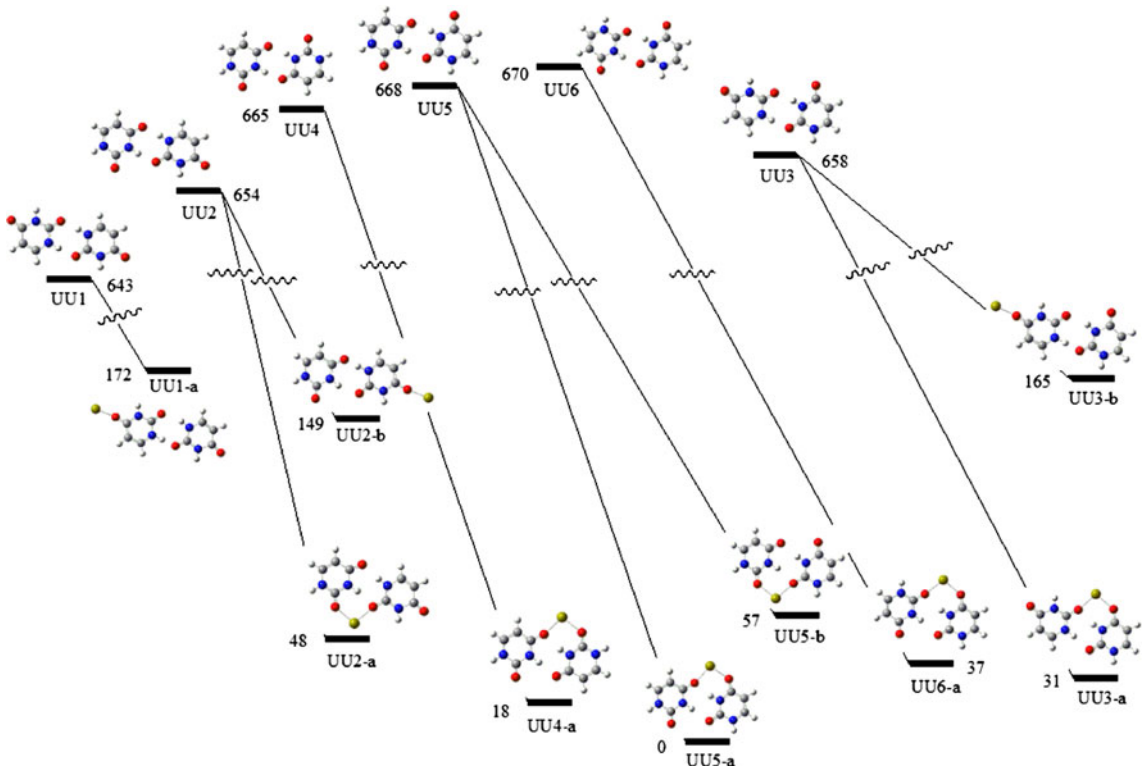

Fig. 2 Structure and relative stability of the six uracil dimers and its more stable Ca^{2+} complexes. All values, in kJ mol^{-1}; are referred to the most stable $(uracil)_2Ca^{2+}$ complex, UU5-a

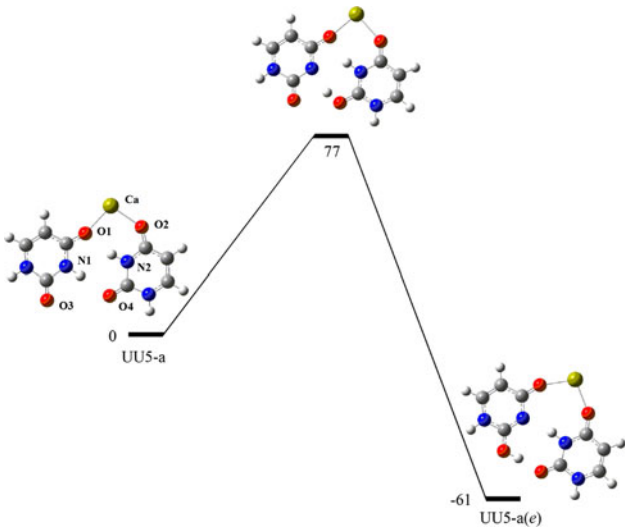

Fig. 3 Activation barriers associated with PT processes within the $(uracil)_2Ca^{2+}$ global minimum UU5-a. All values are in kJ mol^{-1}

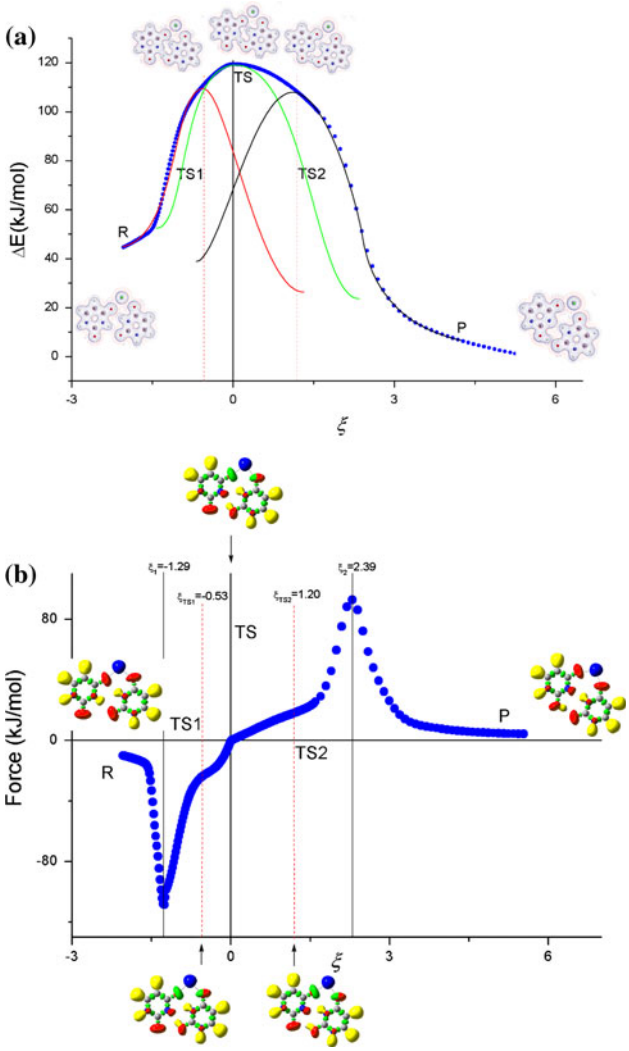

Fig. 4 Energy profile (**a**) and force profile (**b**) for the processes connecting UU5-a with UU5-a(*e*). In figure (a), the energy density for the reactant and the products, as well as for the transition states TS1, TS, and TS2 are shown. In these plots, positive and negative values of the energy density are denoted by *dashed red lines* and *solid blue lines*, respectively

complex corresponds to a dimer between the diketo form of one of uracil moieties and the enolic form of the other. The activation barrier for this process is 77 kJ mol^{-1}, which is significantly lower than the corresponding activation barriers for a similar process in both isolated uracil (197 kJ mol^{-1}) and uracil-Ca^{2+} complex (154 kJ mol^{-1}) [37]. This decrease in the activation barrier points apparently to a catalytic effect triggered by Ca^{2+} association.

However, the structure of the transition state found (see Fig. 3) and the anomalous profile of both the potential energy curve and the curve of the forces along the reaction coordinate (See Fig. 4a, b, respectively, for the UU5a (R) → UU5a(*e*) (P) process), clearly show that a more complicated mechanism than just a single intramolecular PT must be taking place. The shoulder observed in the force in the region previous to the TS as well as the almost linear increase observed after the TS clearly indicate that the process connecting reactants and products is not an elementary one.

This is actually seen when looking at the plots of the energy density and the ELF along the potential energy curve and the forces profile, respectively. The populations of the ELF basins are summarized in Table S2 of the supporting information. In the reactants ($\xi \approx -2$), one clearly observes an ionic interaction between Ca^{2+} and the two (fomamide-like) carbonyl oxygens and two NH···O intermolecular hydrogen bonds. At a more advanced point along the reaction coordinate ($\xi = -0.53$), a PT within the HB not interacting with the metal dication is taking place, and the proton appears almost midway between the N and the O atoms. At this point, the ELF shows the presence of an OH disynaptic basin which did not exist in the reactants, and the disappearance of the NH disynaptic basin. At the same time, the monosynaptic N lone-pair, which in the reactants has a clear π-character, becomes now a monosynaptic basin with a noticeable σ character. This PT process would involve a (hidden) transition state (TS1) which can be qualitatively represented by the red potential energy curve. A further evolution of the system to reach ($\xi = 0$) leads to the aforementioned PT to almost completion. Actually, the transition vector at $\xi = 0$ corresponds to the relative displacement of the right monomer with respect to the left one, to favor the interaction of the (urea-like) carbonyl group of the left monomer with the OH group formed in the first PT. Note that this displacement will also favor the interaction of the NH group of the right monomer with the (deprotonated) N atom of the left one. The OH···O interaction triggers a PT

from the right monomer toward the left one ($\xi = 1.20$). At this point, which will correspond to the hidden transition state (TS2) associated with the OH···O PT (black curve), the proton appears almost midway between the two oxygen atoms. Note that the ELF shows that at this point the PT is not completed since the OH disynaptic basin, although polarized toward the left monomer, is still located at the right monomer. From here, the system evolves toward the products, by completing the aforementioned PT. The consequence is that the right monomer recovers the diketo arrangement and only the left monomer presents an enol group. Hence, although apparently an intramolecular PT took place from the NH group of the left monomer toward one of the (urea-like) carbonyl groups of the same monomer, the real process involves three steps: a) a PT from the NH group of the left monomer toward the (formamide-like) carbonyl group of the right monomer, b) the relative displacement of the right monomer with respect to the left one and c) a PT from the OH group of the right monomer, formed in the first step, toward the (urea-like) carbonyl group of the left monomer.

This is also nicely reflected by looking at the characteristics of the molecular graphs (See Fig. 5) evaluated at the critical points in the evolution of the force (see Fig. 3) and to the work employed in each step.

For the reactant ($\xi \approx -2$), two BCPs are located between Ca^{2+} and the two (formamide-like) carbonyl oxygens of UU5 with small electron densities as in typical ionic interactions. Two NH···O intramolecular HBs are also observed. The work needed to reach $\xi = -1.29$ (23.7 kJ mol^{-1}) is associated with the structural preparation of the system, so that at $\xi = -1.29$ the PT from the NH group of the left monomer has already started, as shown by a significant decrease in the electron density at the N–H BCP and a concomitant increase in the electron density at the O–H BCP. To reach TS1 ($\xi = -0.53$), the work needed (42.7 kJ mol^{-1}) corresponds to the electronic reordering and represent 65% of the activation barrier. When $\xi = -0.53$ is reached, the PT transfer process is practically complete, so that the initial NH···O HB has been replaced by a N···HO HB. On going from ($\xi = -0.53$) toward ($\xi = 0$), the displacement of the right monomer with respect to the left one starts. Obviously, this structural rearrangement requires little work (8.3 kJ mol^{-1}), the main consequence being that the NH group of the right monomer starts forming a HB also with the deprotonated N atom of

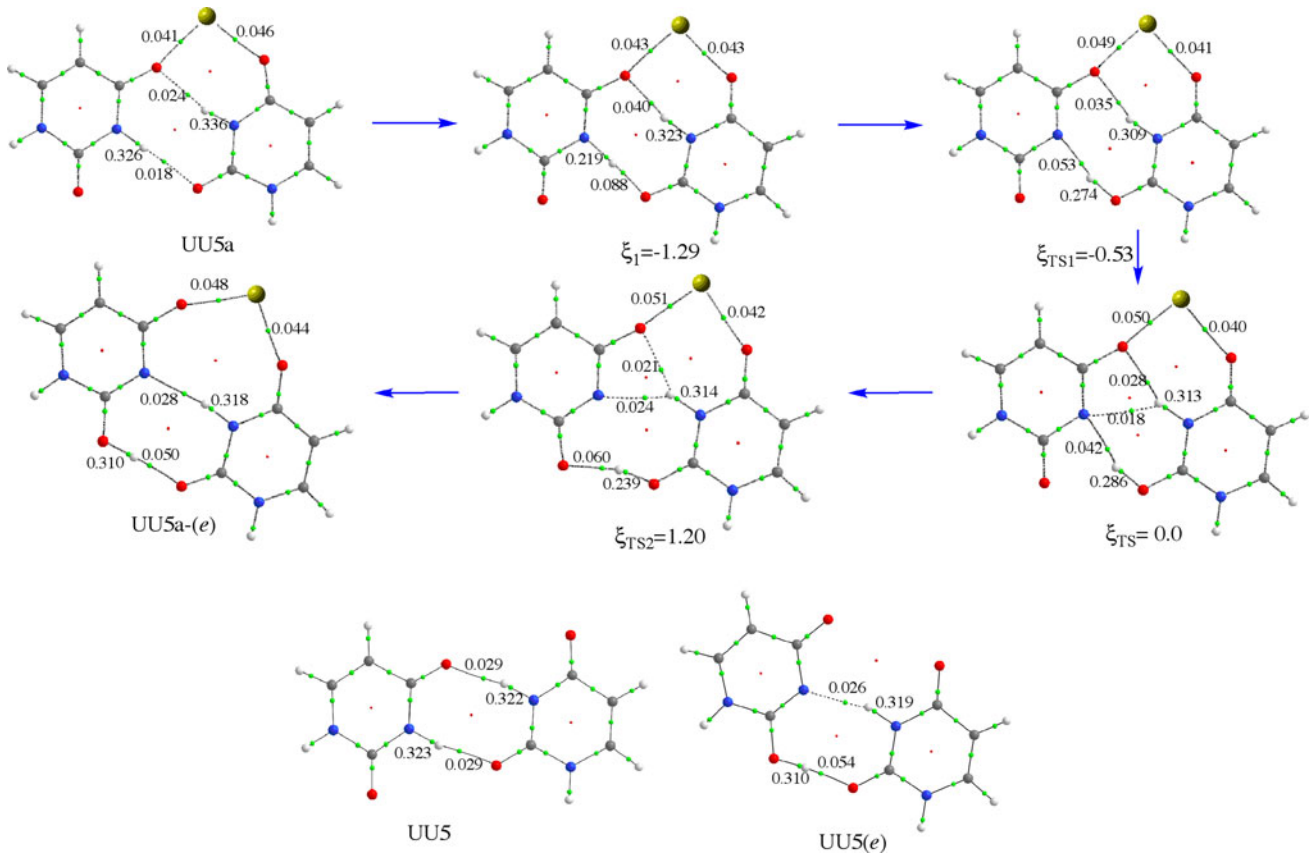

Fig. 5 Molecular graphs along the reaction coordinate connecting UU5-a with UU5-a(*e*). At the bottom of the figure, the molecular graphs for the neutral UU5 and UU5(*e*) compounds are also given for the sake of comparison. Electron densities in a.u

the left monomer. A little further, a second structural reordering, which requires a work of 11.3 kJ mol^{-1} takes place. As a consequence, the OH group of the right monomer starts to interact with the (urea-like) carbonyl group of the left monomer, so that when the TS2 is reached ($\xi = 1.20$) the PT from the OH of the right isomer toward the (urea-like) carbonyl of the left one starts, as evidenced by the decrease in the electron density at the O–H covalent bond and the concomitant increase in the electron density at the OH···O HB. The completion of the PT requires an electronic reorganization work of 47.7 kJ mol^{-1} to reach $\xi = 2.39$, and from here the system relax toward the product, the work involved in this process being 60.4 kJ mol^{-1}.

One question that needs to be answered is what is the possible role of Ca^{2+} on the stabilization of these enol-diketo dimers. As shown in Fig. 3, the enol-diketo dimes, UU5-a(*e*) is more stable than the diketo-diketo one UU5-a. The question is, whether the association with Ca^{2+} is responsible for the enhanced stability of the enol-diketo form. To answer this question, we have calculated the energy of the isolated dimer and the corresponding dimer-Ca^{2+} complex. The results obtained indicate that the isolated enol-diketo form is 64.7 kJ mol^{-1} less stable than the diketo-diketo isomer, whereas for the corresponding Ca^{2+} complexes is the other way around, and UU5-a(*e*) isomer is 61.3 kJ mol^{-1} more stable than UU5-a.

In other words, whereas the PT process from UU5-a to UU5-a(*e*) is exothermic, the corresponding process for the isolated dimers would be clearly endothermic. This can be due to two different effects, the perturbation caused by Ca^{2+} on the HBs connecting both monomers and/or the different basicity of the carbonyl groups interacting with the metal dication. A comparison of the molecular graphs of UU5 and UU5-a (see Fig. 5) clearly indicates that association of Ca^{2+} to the former results in a weakening of both intermolecular hydrogen bonds. This is consistent with the NBO second-order perturbation energies. As shown in Table 1, in UU5 there is an interaction between the two lone-pairs of the carbonyl oxygens with the σ_{NH}* antibonding orbitals, associated with the two intermolecular HBs that are almost identical. Upon Ca^{2+} attachment the upper HB becomes weaker, because the donation from the oxygen lone-pair, which is interacting with Ca^{2+}, toward the σ_{NH}* antibonding orbital drastically decreases. The strength of the lower HB decreases more, because, on the one hand, the donating capacity of the carbonyl oxygen decreases upon Ca^{2+} attachment and the intrinsic acidity of the NH group also decreases. In UU5(*e*), the first N2H···O1 HB in UU5 is replaced by a N2H···N1 HB. Similarly, the N1H···O4 HB is replaced by a stronger O3H···O4 HB, because the OH group is a stronger HB donor than the NH one. The important finding however is that the former becomes reinforced upon Ca^{2+} association due likely to the enhanced acidity of the NH groups and the latter weakens only slightly, due likely to a slightly decrease in the basicity of the carbonyl group. The second important factor which may explain the enhanced stability of the enol-keto dimers upon Ca^{2+} association is that in these complexes the metal cation interacts with two free carbonyl groups, whereas in the diketo-diketo complexes, one of the interactions involves the carbonyl group which is already acting as HB acceptor in one of the NH···O intermolecular HBs.

Table 1 Second-order interaction energies (in kJ mol^{-1}) between the HB acceptor lone-pair and the σ_{XH}* (X = N, O) antibonding orbital in UU5, UU5-a, UU5(*e*), and UU5-a(*e*) systems

	UU5	UU5-a		UU5(*e*)	UU5-a(*e*)
$LP_{O1} \rightarrow \sigma_{N2H}$*	37/41[a]	36/12[a]	$LP_{N1} \rightarrow \sigma_{N2H}$*	67	77
$LP_{O4} \rightarrow \sigma_{N1H}$*	37/40[a]	28/13[a]	$LP_{O4} \rightarrow \sigma_{O3H}$*	57/118	56/100[a]

[a] The two values reported correspond to the interactions of the two lone-pairs of each carbonyl oxygen

5 Conclusions

Although in uracil dimers PT occurs as an almost synchronous double PT processes that connect the diketo dimer with a keto-enol dimer, the process within the most stable (uracil)$_2Ca^{2+}$ complexes is much more complicated, and the product of the reaction looks like the result of an intramolecular PT from one of the NH groups of one monomer to one of the carbonyl groups of the same monomer. However, an analysis of the force profile shows that the intimate mechanism implies three elementary steps, two of which, the first and the third steps, are intermolecular PT and the second an in-plane displacement of one monomer with respect to the other. The result of this so-called assisted intramolecular proton transfer is the formation of a dimer in which only one monomer is a keto-enol derivative, the other monomer being apparently unchanged, although it suffers significant structural rearrangements along the reaction coordinate. Quite importantly, this dimer is significantly stabilized upon Ca^{2+} association, therefore, while the most stable uracil dimers correspond systematically to associations involving only the diketo forms, in (uracil)$_2Ca^{2+}$ complexes the most stable structures correspond to those in which one of the monomers is a keto-enol uracil isomer. The origin of this enhanced stability is likely twofolded: (1) a reinforcement of the HBs connecting the monomers upon Ca^{2+} association and (2) a stronger interaction of the doubly charged metal ion with the dimer, because the interaction involves carbonyl groups not engaged in the intermolecular hydrogen bonds.

The activation barriers, associated with this intradimer enolization process in (uracil)$_2$Ca^{2+} complexes, are lower than those calculated for the double proton transfer process in the neutral (uracil)$_2$ dimers and much lower than those calculated for the tautomerization within each monomer. Hence, these assisted intramolecular PT may play a quite significant role in the tautomerization of uracil and likely also in the tautomerization of uracil derivatives.

Acknowledgments This work has been partially supported by the DGI Project No. CTQ2009-13129-C01, by the Project MADRISOLAR2, Ref.: S2009PPQ/1533 of the Comunidad Autónoma de Madrid, by Consolider on Molecular Nanoscience CSC2007-00010, and by the COST Action CM0702. A generous allocation of computing time at the CCC of the UAM is also acknowledged.

References

1. Watson JD, Crick FHC (1953) Nature 171:964–967
2. Watson JD, Crick FHC (1953) Nature 171:737–738
3. Shibata M, Zielinski TJ, Rein R (1990) Theoretical Biochemistry and Molecular Biophysics. Adenine Press, New York
4. Saenger W (1984) Principles of Nucleic Acid Structure. Springer Verlag, New York
5. Jeffrey GA, Saenger W (1991) Hydrogen Bonding in Biological Structure. Springer Verlag, New York
6. Nelson DL, Cox MM, Lehninger AL (2000) Principles of Biochemistry. Worth Publishers Inc, New York
7. Kierdaszuk B, Stolarski R, Shugar D (1983) Eur J Biochem 130:559–564
8. He L, Kierzek R, Santalucia J, Walter AE, Turner DH (1991) Biochemistry 30:11124–11132
9. Florian J, Hrouda V, Hobza P (1994) J Am Chem Soc 116:1457–1460
10. Walter AE, Wu M, Turner DH (1994) Biochemistry 33:11349–11354
11. Douhal A, Kim SK, Zewail AH (1995) Nature 378:260–263
12. Florian J, Leszczynski J (1996) J Am Chem Soc 118:3010–3017
13. Chen XY, McDowell JA, Kierzek R, Krugh TR, Turner DH (2000) Biochemistry 39:8970–8982
14. Jiang LH, Russu IM (2001) Nucleic Acids Res 29:4231–4237
15. Kryachko ES (2002) Int J Quant Chem 90:910–923
16. Gorb L, Podolyan Y, Dziekonski P, Sokalski WA, Leszczynski J (2004) J Am Chem Soc 126:10119–10129
17. Zoete V, Meuwly M (2004) J Chem Phys 121:4377–4388
18. Noguera M, Sodupe M, Bertran J (2004) Theor Chem Acc 112:318–326
19. Rak J, Makowska J, Voityuk AA (2006) Chem Phys 325:567–574
20. Noguera M, Sodupe M, Bertran J (2007) Theor Chem Acc 118:113–121
21. Noguera M, Bertran J, Sodupe M (2008) J Phys Chem B 112:4817–4825
22. Zhang JD, Chen ZF, Schaefer HF (2008) J Phys Chem A 112:6217–6226
23. Czerminski R, Lesyng B, Pohorille A (1979) Int J Quant Chem 16:605–613
24. Les A, Ortegablake I (1986) Int J Quant Chem 30:225–237
25. Katritzky AR, Karelson M, Harris PA (1991) Heterocycles 32:329–369
26. Leszczynski J (1992) J Phys Chem 96:1649–1653
27. Estrin DA, Paglieri L, Corongiu G (1994) J Phys Chem 98:5653–5660
28. Leszczynski J, Sponer J (1996) J Mol Struct Theochem 388:237–243
29. Lamsabhi M, Alcamí M, Mó O, Bouab W, Esseffar M, Abboud JLM, Yáñez M (2000) J Phys Chem A 104:5122–5130
30. Marino T, Russo N, Sicilia E, Toscano M (2001) Int J Quant Chem 82:44–52
31. Millefiori S, Alparone A (2004) Chem Phys 303:27–36
32. Trujillo C, Mó O, Yáñez M (2007) Org Biomol Chem 5:3092–3099
33. Feyer V, Plekan O, Richter R, Coreno M, Vall-Ilosera G, Prince KC, Trofimov AB, Zaytseva IL, Moskovskaya TE, Gromov EV, Schirmer J (2009) J Phys Chem A 113:5736–5742
34. Lamsabhi AM, Mó O, Gutiérrez-Oliva S, Perez P, Toro-Labbé A, Yáñez M (2009) J Comput Chem 30:389–398
35. Lamsabhi AM, Alcamí M, Mó O, Yáñez M, Tortajada J (2006) J Phys Chem A 110:1943–1950
36. Gutle C, Salpin JY, Cartailler T, Tortajada J, Gaigeot MP (2006) J Phys Chem A 110:11684–11694
37. Trujillo C, Lamsabhi AM, Mó O, Yáñez M, Salpin JY (2008) Org Biomol Chem 6:3695–3702
38. Sponer J, Sabat M, Burda JV, Leszczynski J, Hobza P (1999) J Phys Chem B 103:2528–2534
39. Zhang Y, Huang KX (2007) J Mol Struct Theochem 812:51–62
40. Miyachi H, Matsui T, Shigeta Y, Hirao K (2010) Phys Chem Chem Phys 12:909–917
41. Lee C, Yang W, Parr RG (1988) Theochem 40:305–313
42. Becke AD (1993) J Chem Phys 98:5648
43. Corral I, Mó O, Yáñez M, Scott A, Radom L (2003) J Phys Chem A 107:10456–10461
44. van der Wijst T, Guerra CF, Swart M, Bickelhaupt FM (2006) Chem Phys Lett 426:415–421
45. Toro-Labbe A (1999) J Phys Chem A 103:4398–4403
46. Jaque P, Toro-Labbe A (2000) J Phys Chem A 104:995–1003
47. Gutierrrez-Oliva S, Herrera B, Toro-Labbe A, Chermette H (2005) J Phys Chem A 109:1748–1751
48. Politzer P, Toro-Labbe A, Gutierrez-Oliva S, Herrera B, Jaque P, Concha MC, Murray JS (2005) J Chem Sci 117:467–472
49. Toro-Labbe A, Gutierrerez-Oliva S, Murray JS, Politzer P (2007) Mol Phys 105:2619–2625
50. Rincon E, Toro-Labbe A (2007) Chem Phys Lett 438:93–98
51. Bader RFW (1990) Atoms in Molecules. A Quantum Theory. Clarendon Press, Oxford
52. Becke AD, Edgecombe KE (1990) J Chem Phys 92:5397–5403
53. Silvi B, Savin A (1994) Nature 371:683–686
54. Keith TA (2010) AIMAll (Version 10.05.04). http://aim.tkgristmill.com
55. Savin A, Nesper R, Wengert S, Fäsler TF (1997) Angew Chem Int Ed Engl 36:1808–1832
56. Mó O, Yáñez M, Martín Pendás A, Del Bene JE, Alkorta I, Elguero J (2007) Phys Chem Chem Phys 9:3970–3977
57. Noury S, Krokidis X, Fuster F, Silvi B (1999) Comput Chem 23:597–604
58. Reed AE, Curtiss LA, Weinhold F (1988) Chem Rev 88:899–926
59. Kelly REA, Kantorovich LN (2006) J Phys Chem B 110:2249–2255